Vol. 46, No. 1 (2024) 151-162, DOI: 10.24874/ti.1568.11.23.01

Tribology in Industry

www.tribology.rs

RESEARCH

Enhancement of Wear Resistance of High-Load Pressing Screw in Smokeless Charcoal Production by Using Genetic Algorithm and Discrete Element Method

Hong Tien Nguyen[a,*], Tuan-Linh Nguyen[a], Nguyen Van Thien[b], Phan Van Quoc[c]

[a]*School of Mechanical and Automotive Engineering, Hanoi University of Industry, Vietnam,*
[b]*Organization - administration department, Hanoi University of Industry, Vietnam,*
[c]*DENSO Manufacturing Viet Nam Co. Ltd, Vietnam.*

Keywords:

Pressing screw
DEM
EDEM
Simulation
Smokeless

* Corresponding author:

Hong Tien Nguyen
Email: nguyenhongtien@haui.edu.vn

Received: 2 November 2023
Revised: 21 December 2023
Accepted: 23 January 2024

A B S T R A C T

During the production of smokeless charcoal, the pressing screw of the sawdust compressor is exposed to the effects of friction and elevated temperature, resulting in rapid wear. This phenomenon not only diminishes productivity but also exerts adverse influences on the final product's quality. Consequently, the pursuit of research endeavors aiming at prolonging the lifespan of the pressing screw holds significant importance, not only in reducing production costs but also in enhancing the product's overall quality. This paper adopts an innovative approach by integrating theoretical calculations, numerical simulations with practical experiments to ascertain the optimal profile for the pressing screw. This methodology employs Genetic Algorithm and Discrete Element Method (DEM) simulations in conjunction with the EDEM software to simulate the working process and provide the optimal profile of the pressing screw. The analysis and simulation results indicate a substantial enhancement in the wear resistance of the pressing screw while ensuring the efficient movement of discrete materials during the pressing process. The results of this study not only indicate the main wear locations on the pressing screw but also suggest the optimal profile, providing a basis and control for wear assessment. Furthermore, the results of this research not only identifies the principal areas that are susceptible to wear on the pressing screw but also proposes optimal profile, threreby establish a solid foundation and methodology for wear assessment. These results will be pragmatically implemented in smokeless charcoal production factories, concurrently pave the way for further research and applications in this field.

1. INTRODUCTION

In the smokeless charcoal production industry, the role of pressing screw with its helical surface plays a crucial role in the movement, compressing sawdust, generating friction, maintaining temperature, preventing wear, and ensuring the efficient movement of discrete material flows.

The helical surface of the pressing screw is available in a range of configurations, including helical, U-thread, and V-thread designs. These configurations serve specific purposes, which include facilitating the movement and transportation of sawdust, generating compression pressure, and maintaining optimal temperatures. Throughout the sawdust pressing process, the pressing screw can adopt straight, circular, helical, or occasionally cycloidal profiles. Determining the optimal configuration of the pressing screw during operation presents a considerable challenge due to the intricate and multifaceted nature of this process. It is vital to determine the suitable alignment between the pressing screw and the flow of discrete materials. This alignment is of utmost importance as it significantly reduces friction, improves wear resistance, and extends the lifespan of the pressing screw. This optimized configuration substantially supports the movement and compression of materials, ultimately resulting in the production of high-quality pressed sawdust bars.

Currently, there are several studies in this field. Author Gerald Muller [1] has developed a theoretical model describing the shape of the screw and has effectively integrated it with previous experimental research results. However, this work mainly focuses on researching the performance of the Archimedean screw. In the research paper [2], author Matus Milos has studied and proposed some suitable profiles for manufacturing the pressing screw in the sawdust compressor. Nevertheless, this research remains a work in progress, requiring time to verify the results and primarily concentrates on the pressure that the pressing screw must withstand, without addressing other influences such as temperature and wear of the pressing screw. In the research [3], authors Krizan Peter and Svátek Michal explored the effects of several parameters (including temperature, moisture content of the input material, pressing pressure, size of the raw material particles) on the compression density of the sawdust products. However, this research group exclusively focused on investigating the parameters influencing the quality of the compressed pellets and applied it solely to the sawdust pressing process, excluding parameters related to other types of sawdust. In the research paper [4], author A. Gaspar-Cunha and colleagues developed a multi-objective evolutionary algorithm (MOEA) to establish operational conditions and determine the shape of a single plastic pressing screw. Although this work modeled the single screw pressing process as a multi-objective optimization problem with the goal of optimizing performance, it did not focus on other materials of the pressing screw and did not study the flow of discrete materials. In the research project [5], D. Kretz and the research team used Blender software to simulate and predict the flow of discrete materials. Although this simulation tool could predict processes with various screw types, it did not incorporate the process of pressing discrete materials. The research paper [6] by Milada Pezo and colleagues investigated the influence of the geometric length of the screw on the product quality using the discrete element method (DEM). In this study, they mixed zeolite with sand and explored the impact of the screw length, particle diameter, and shape changes to improve the quality of that material mixture. However, it is important to underscore that increasing the speed and displacement of the particles would erode the screw and reduce its lifespan.

To date, there have been studies on the optimization of pressing screw profiles, but no research endeavors have comprehensively addressed the issue of pressing screw wear during operation, nor have any solutions been proposed to augment the longevity of pressing screw in the smokeless charcoal production industry. Furthermore, the amalgamation of simulation methodologies with cutting-edge design approaches is demonstrating profound advantages, particularly within the mechanical manufacturing sector. The simulation process entails the creation of models and experimentation conducted under conditions that closely mimic real-world scenarios. The outcomes derived from these simulation processes are subsequently employed to formulate or refine real-world systems. Investigating the impact of technological parameters on pressing screw wear is instrumental in the selection of appropriate technological settings to mitigate wear and extend the operational lifespan of pressing screw. This interdisciplinary approach, in conjunction with simulation methodologies, is

garnering significant attention from domestic and global scientific community.

The integration of design methodologies with simulation techniques represents a rational approach in the domain of pressing screw design for smokeless charcoal production. Through the utilization of simulation, we can thoroughly assess and evaluate design variations prior to actual experimentation. This approach not only conserves time, effort, and financial resources but also mitigates risks and expenses throughout the developmental process. Leveraging the advantages of simulation, this methodology furnishes a comprehensive and profound comprehension of the performance and capabilities of pressing screw in the context of smokeless charcoal production. Consequently, it contributes to process optimization and the enhancement of final product quality.

This paper is meticulously crafted with the objective of investigating appropriate pressing screw profile in conjunction with simulation solutions utilizing Altair EDEM software for discrete materials. The goal is to mitigate wear and prolong the operational lifespan of the pressing screw. The outcomes and simulation models derived from this study can be applied in smokeless charcoal production facilities to elevate efficiency and refine the production process.

2. MATERIALS AND METHODS

2.1 Materials

The materials commonly used for pressing screw are carbon-based, with the steel grade C45 being a prevalent choice. Equivalent steel grades include 1045, S45C, and 080M46. According to Vietnamese standards, C45 steel has chemical composition as shown in Table 1.

Table 1. Chemical composition of C45 steel.

Steel grade	Content of elements %						
	C	Si	Mn	P	S	Cr	Ni
				No greater than			
C45	0,42÷0,50	0,17÷0,37	0,5÷0,8	0,04	0,04	0,25	0,25

Screws used in the production of smokeless charcoal typically have a structure as shown in Figure 1.

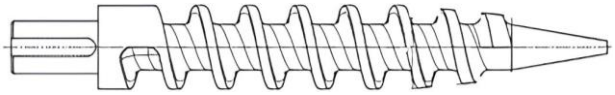

Fig. 1. The structure of a pressing screw.

The primary constituents of sawdust in smokeless charcoal production are Cellulose, Lignin, Hemicellulose, and water. Among these, Cellulose comprises a substantial portion of sawdust, serving as the primary constituent of wood and forming the fibrous structure within sawdust. Lignin, conversely, is a flexible insoluble material in wood, constituting a smaller fraction of sawdust but playing a vital role in its structure and hardness. Hemicellulose, a component of wood fiber, is more water-soluble than cellulose. The arrangement and proportion of these constituents in sawdust can vary based on the wood type and the product manufacturing process. Through analysis, as depicted in Figure 2, sawdust is observed to have an irregular shape with dimensions ranging from 0.08 to 0.6 mm in length and width.

Fig. 2. The image of sawdust in smokeless charcoal production.

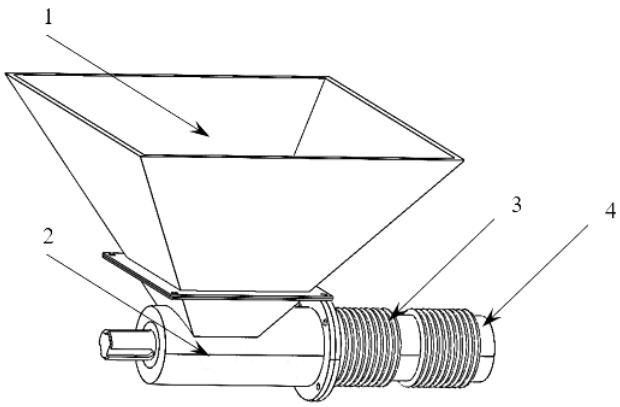

Fig. 3. The pressing principle of the sawdust compressor.

When sawdust is fed through loading funnel 1, it is guided into the clearance section, where a series of threads 2 (material guides) transfer the material to the pressing thread section (pressing screw 3, consisting of 3 threads). In this pressing section, the material is compressed under high pressure and temperature to create bonding, and it is then extruded through the die 4 to form compressed pellets as the final product.

2.2 Method

a) Discrete Element Method (DEM) foundations

In the realm of simulating Discrete Element Method (DEM), there are two primary methods to depic material behavior: the continuous method and the discrete method. The discrete method serves as a robust approach for simulating individual particles as distinct entities. In this method, materials are represented as a collection of particles, in which each particle represent a unified entity in the system. The behavior of the entire system depends on the interactions among these individual particles.

The discrete method proves particularly useful when studying phenomena occurring at the particle diameter scale and when aiming to simulate the overall behavior of particles. This is an ideal choice for systems containing individual particles, especially when investigating interactions at the particle level and phenomena at the particle diameter scale. For irregularly shaped sawdust particles, each individual particle is modeled as a distinct entity, and the discrete material is represented as an idealized aggregation of these particles in a spherical shape, as shown in Figure 4. The behavior of the entire system relies on the interactions between each individual particle. The discrete approach is an efficient approach to study phenomena occurring at the particle diameter scale and simulate the overall behavior of particles [7-12].

These principles are also applicable in three-dimensional space and for contacts between particles and various geometric shapes. This ensures that modeling for calculation and simulation can be flexibly and accurately applied in numerous situations and different spaces. Utilizing the discrete method in simulating discrete materials not only aids in comprehending phenomena occurring at the particle diameter scale but also offers a precise insight into the overall behavior of the system, establishing the groundwork for numerous studies in this field.

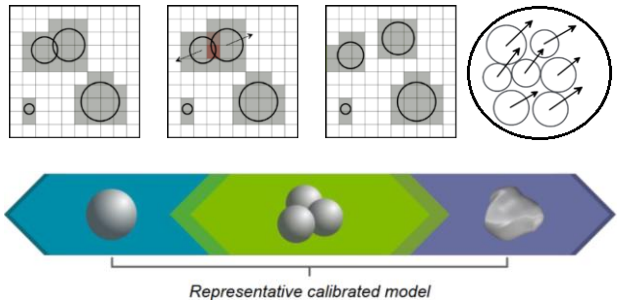

Fig. 4. Principles of Discrete Element Method simulation.

b) Foundation for pressing screw wear calculation

The wear of the pressing screw can be calculated based on the mass deviation ratio of the pressing screw before and after working compared to the initial mass of the pressing screw, as per the experimental formula (1).

$$W = \frac{M - M_1}{M} \quad (1)$$

Through numerical simulation, we can rely on simulated wear to assess the wear mass at the surveyed location determined by formula (2) and evaluate the wear compared to reality.

$$M_w = d_w . A_1 . m \quad (2)$$

Where M_w - Wear mass

d_w (mm) represents the wear depth calculated by formula (3).

A_1 - Wear surface area (mm^2)

m - Material density of the pressing screw (kg/mm^3)

Here, the wear depth d_w can be calculated as follows:

$$d_w = \frac{g(\alpha)E(\alpha)m_P}{A} \text{ mm} \quad (3)$$

In which E(α) is wear volume per unit mass determined by formula (4) [13-16].

$$E(\alpha) = 65W^{-k_1}\left(\frac{v}{104}\right)^{2.3H_v^{0.038}}\left(\frac{D}{0.326}\right)^{0.19} \quad (4)$$

In which g(α) is the coefficient depending on the impact angle affecting the wear, calculated by formula (5).

$$g(\alpha) = \sin(\alpha)^{0.71H_v^{0.14}} (1 + H_v(1 - \sin(\alpha))^{2.4H_v^{-0.94}} \quad (5)$$

Where A - geometry element area (mm²)

m_p - particle mass (kg)

α - particle impact angle (rad)

v - particle impact velocity (m/s)

D - particle diameter (mm)

H_v - Vickers hardness of worn material (GPa)

W - Material wear constant

ΔU - particle sliding distance at contact (m)

Material wear constant W_{0ka} where: $W_{0ka} \approx 3$ for carbon steel [15,17,18].

During the material pressing process, sawdust particles are conveyed from the feeding chamber and interact with the surface of the guiding screw, move along the screw axis of the pressing screw. When they come into contact with the guiding region, where there is no significant increase in temperature and pressure, the material particles may move at a velocity V at an angle α relative to the transverse direction. This leads to surface wear of the screw. For easy calculation, we can divide it into two perpendicular velocity components: Vt and Vn. Depending on the velocity and direction of motion, the screw may experience abrasion and result in surface wear, rather than plastic deformation. This process is modeled in Figure 5.

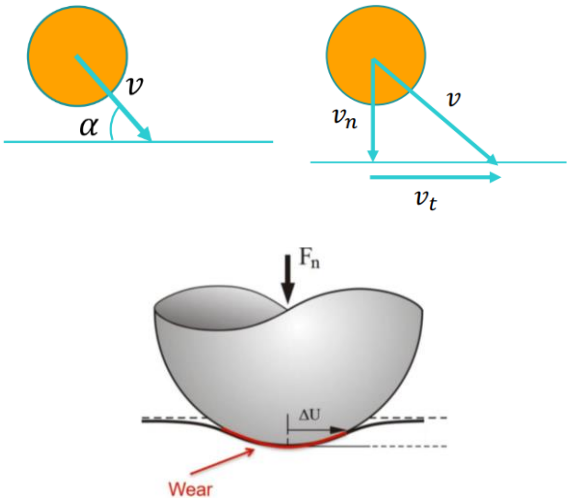

Fig. 5. Wear model of pressing screw in interaction with discrete materials.

The wear of a pressing screw can significantly reduce its lifespan, leading to the need for premature replacement and causing disruptions in the production process. In an effort to address these challenges, this paper proposes an optimized pressing screw design approach. The objective is to enhance the lifespan of the pressing screw during operation, minimize the frequency of equipment replacement, and improve the overall efficiency of the production system.

3. OPTIMIZING THE PRESSING SCREW PROFILE BASED ON VOLUME AND PRESSURE CRITERIA

The operational process of pressing screws in smokeless charcoal production imposes specific requirements to ensure its efficiency, including compression pressure, compression volume, temperature, and pressing time... Among these criteria, pressure and volume play a pivotal role in the wear of the pressing screw. Therefore, the key challenge lies in designing the pressing screw profile which can facilitate rapid pressure increasingly on the material, reduce friction between the material flow and the pressing screw, and ensure the seamless movement of the material. The optimization of the pressing screw profile is built on the basis of the Genetic Algorithm (GA), as depicted in Figure 6.

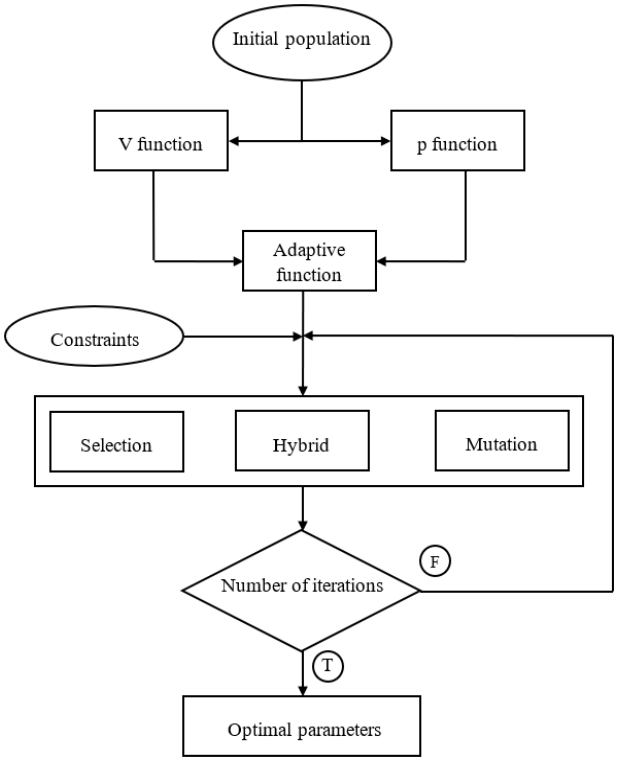

Fig. 6. Optimized pressing screw profile block diagram.

a) Press Volume V

Assuming that the space between the anterior shape, the bottom shape, and the posterior shape of the screw groove is filled with material, then the volume of this space is precisely the volume of the material transported through a unit longitudinal cross-section, as shown in Figure 7.

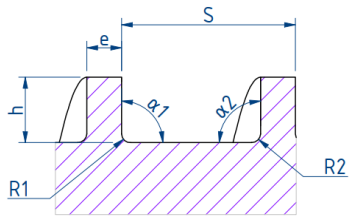

Fig. 7. Longitudinal cross-section of the pressing screw profile.

Where:

α_1, α_2: front and rear angles

R_1, R_2: radius of the front and rear angles

s: pitch of the screw

e: width of the screw thread crest

h: depth of the screw thread groove

Let V be the volume of the material filled in the pressing chamber, D be the outer diameter of the screw, and i be the number of screw threads. We can calculate the ratio $\frac{V}{\pi D^3}$ as follows [2]:

$$\frac{V}{\pi D^3}=(1-\frac{h}{D}).\frac{h}{D}\left[\frac{s}{D}.(1-\frac{i.e}{s})+\frac{1}{2}.\frac{\sin(\alpha_1+\alpha_2)}{\sin\alpha_1.\sin\alpha_2}\right]-\left[\frac{1}{2}.\frac{h}{D}-\left(\frac{h}{D}\right)^2+\frac{2}{3}\left(\frac{h}{D}\right)^3\right].\frac{\sin(\alpha_1+\alpha_2)}{\sin\alpha_1.\sin\alpha_2}$$
$$-\left(1-\frac{2h}{D}\right).\left(\frac{r_1}{D}\right)^2.\left[\frac{1-\cos\alpha_1}{\sin\alpha_1}-\frac{\pi}{360}.(180-\alpha_1)\right]-\left(1-\frac{2h}{D}\right).\left(\frac{r_2}{D}\right)^2.\left[\frac{1-\cos\alpha_2}{\sin\alpha_2}-\frac{\pi}{360}.(180-\alpha_2)\right] \quad (6)$$
$$-\frac{1}{6}.\left(\frac{r_1}{D}\right)^3.\left[\frac{10\sin\alpha_1-\sin2\alpha_1}{1-\cos\alpha_1}-\frac{\pi}{30}.(180-\alpha_1)\right]-\frac{1}{6}.\left(\frac{r_2}{D}\right)^3.\left[\frac{10\sin\alpha_2-\sin2\alpha_2}{1-\cos\alpha_2}-\frac{\pi}{30}.(180-\alpha_2)\right]$$

In the special case, if $\alpha_1=\alpha_2=\frac{\pi}{2}$ or $\frac{R_1}{D}=\frac{R_2}{D}\to 0$, we have: $\frac{V}{\pi D^3}=(1-\frac{h}{D}).\frac{h}{D}.\left[\frac{s}{D}(1-\frac{i.e}{s}\right]$ (7)

So: $V=\pi.h(D-h)(s-i.e)$ (8)

Therefore, it is possible to alter the profile in the longitudinal direction of the screw axis by modifying one of the following parameters:

- Changing the outer diameter (making the screw conical),
- Changing the depth of the screw groove (making the core screw conical),
- Changing the screw pitch.

These parameters can also be adjusted simultaneously to achieve an appropriate compression ratio. The ratio of the volume of the screw groove to the volume of the material passing through it is referred as the compression ratio

$$k=\frac{V}{V_i} \quad (9)$$

b) Compression Pressure

The compression pressure is determined by the following formula [2]:

$$P_n=p_0.e^{A.\frac{l}{d}} \quad (10)$$

In which: p_0 – initial pressure

l – length of the screw, when l = 0 then $p = p_0$

A – proportional factor [2]

$$A=\frac{f_p}{\frac{h}{D}tg\alpha_p\cos\alpha_0\frac{D-h}{D}}[\cos\varphi-f_z\sin\varphi-tg\alpha_p(\sin\varphi-f_z\cos\varphi)$$
$$-\frac{2f_z}{\frac{s}{D}(1-\frac{i.e}{s})\sin\alpha_0\cos\alpha_0}-\frac{f_z\frac{D-2h}{D-h}}{\frac{h}{D}\cos\alpha_0 tg\alpha_z} \quad (11)$$

fp, fz – coefficient of friction between the material and the chamber and the coefficient of friction between the material and the screw correspondingly

φ - coefficient of friction angle

Angles α_p, α_0 và α_s – correspondingly are the angles on the pressing screw geometry corresponding to the length π.D, π.(D–h) and π.(D- 2h), illustrated in Figure 8.

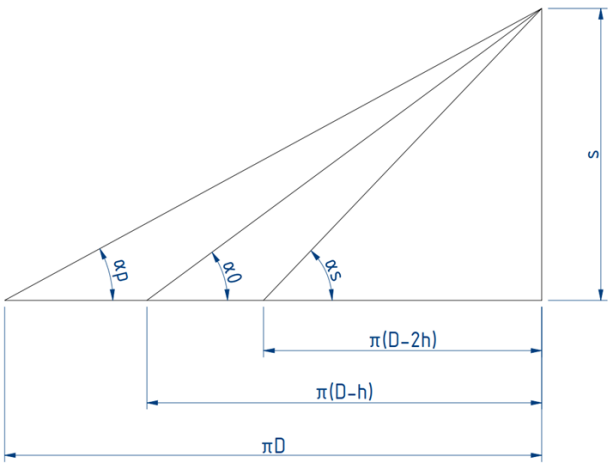

Fig. 8. The step angle on the pressing screw.

From Figure 7, we have:

$$tg\alpha_p = \frac{s}{\pi D} \quad (12)$$

$$tg\alpha_0 = \frac{s}{\pi(D-h)} = tg\alpha_p.\frac{1}{1-\frac{h}{D}} \quad (13)$$

$$tg\alpha_s = \frac{s}{\pi(D-2h)} = tg\alpha_p.\frac{1}{1-\frac{2h}{D}} \quad (14)$$

With the diameter D of the pressing screw determined by the formula (15).

$$D = \left(\frac{Q}{37{,}7.k_v.k_c.k_n}\right)^{2/5} \quad (15)$$

Where the productivity Q of the pressing screw (tons/hour) is determined by the formula (16).

$$Q = 60.\frac{\pi D^2}{4}.t.n.\rho.l.k_c.k_n \quad (16)$$

Where:

D - Screw diameter (mm)

t - Screw pitch (mm)

$t \approx 0.8D$ (17)

Density of the transported material (kg/mm^3)

For sawdust, k_v = 60 [19,20].

The mentioned k_c values can be increased by 1.5 to 2 times for short screws without intermediate bearings. However, when transporting fragile materials, k_c values are reduced.

Coefficient depends on the screw inclination angle, which can be obtained from Table 2 [19,20].

Table 2. Inclination angle parameters.

Inclination angle β	0	5	10	15	20
k_n	1	0,9	0,9	0,7	0,65

After determining the diameter of the conveyor screw D, we proceed to calculate the number of revolutions of the screw shaft n, which is determined according to formula (18).

$$n = \frac{k_v}{\sqrt{D}} \quad (18)$$

For horizontal screws, the power (kW) on the conveyor screw shaft is determined by the following formula [19,20]:

$$P = c_0.\frac{QL}{360} = F.\omega \quad (19)$$

$$P_n = \frac{F}{A} \quad (20)$$

Where:

Q - Material conveying capacity (kg/h)

L - Horizontal conveying length of the material (mm)

H - Vertical conveying height of the material (mm)

C_0 = 1,2 - The coefficient of resistance

P_n - Compression pressure

A - Contact area between the screw and the discrete material

ω - Angular velocity of pressing screw

Optimizing the compression screw profile according to the two criteria of compression volume and compression pressure, assuming that the compression screw profile is considered as an objective function depending on the compression volume and compression pressure, it can be seen that when the volume is increased, The pressing chamber will increase productivity but reduce pressure, and vice versa, increasing pressure will create a good connection between discrete material particles but reduce volume and increase friction, leading to faster wear of the pressing screw. Clearly, these are two opposing objectives. We will put both desired goals into the objective function M according to the weighting method [20].

$$M = w_1.\frac{V}{V^*} + w_2.\frac{P_n}{P_n^*} \rightarrow Max \quad (21)$$

Where w_1 and w_2 are weights satisfying $w_1 + w_2 = 1$.

With V* and Pn* being the volume and pressure limits determined according to the actual working conditions of the pressing screw at the production facility, V* = 20,000 mm3, p* = 113 MPa.

Construct the optimization problem applying the Genetic Algorithm (GA), considering the design variables $X = [\alpha_1, \alpha_2, R_1, R_2, h]^T = [x_1, x_2, x_3, x_4, x_5]^T$ as individuals and forming an initial

population. Then, cross-breeding is carried out to achieve reliability of results, the mutation rate is selected to be between 2% and 4%, the mutation percentage is in the range 2% to 5%, cross-population percentage from 60% to 80%. To achieve that results, 800 generations are needed.

After programming on MATLAB software with the Otimization Tool/Multiobjective Optimization using Genetic Algorithm module, we obtained the results as shown in Table 3.

Table 3. Optimal results on Matlab software.

Parameter	α_1	α_2	R_1	R_2	h
Optimal results	90°	90°	10	10	12

Based on the calculations, we have selected the optimal profile of the pressing screw as shown in Figure 9.

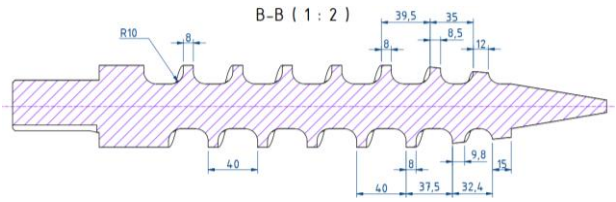

Fig. 9. Optimal profile of the pressing screw.

4. RESULT AND DISCUSSION

a) The dimensions of the factory pressing screw and the optimal pressing screw

After obtaining the optimal calculation results, we proceeded to simulate and compare them with the real production factory pressing screw in Vietnam, with the dimension parameters represented as in Figure 10.

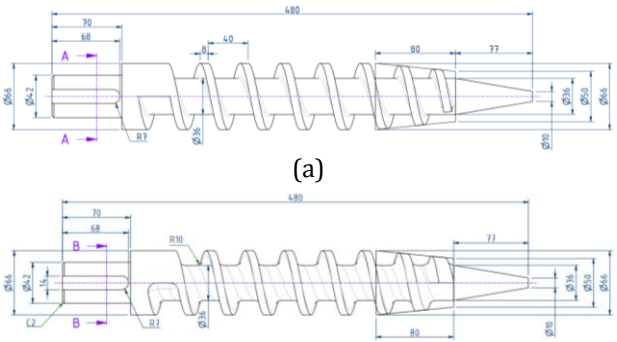

(a)

(b)

Fig. 10. Factory pressing screw (a) and optimal pressing screw (b).

The most significant distinction between the Factory Pressing Screw and the Optimal Pressing Screw lies in the gradual increase in the crest width of the screw starting from the 3rd thread with 8 mm and reaching its maximum size at the end of the pressing screw, measuring 15 mm as indicated in Table 4.

Table 4. The dimensions of the factory pressing screw and the optimal pressing screw.

Parameter	**D (mm)**	**L (mm)**	**D_0 (mm)**	**a_1**	**a_2**	**r_1 (mm)**	**r_2 (mm)**	**h (mm)**	**Screw threads (mm)**	**e_1 (mm)**	**e_2 (mm)**	**e_3 (mm)**	**e_4 (mm)**
Factory pressing screw	66	480	50	90°	90°	10	10	12	40	8	8	8	8
Optimal pressing screw	66	480	50	90°	90°	2	2	12	39.5	15	12	9.8	8.5

We conducted a study on the wear of two pressing screws using numerical simulation methods in Altair software. In real conditions, the pressing screw becomes worn after approximately from 40 to 50 hours of operation, making it unable to extrude materials any further, making it unable to extrude materials any further. The simulation problem could only be carried out for a limited amount of time, and it was accelerated by using a scaling factor of 3600 to convert simulation time to real time.

b) Simulation setup on Altair software

Accurately determining the material model to include in numerical simulation is crucial and directly affects the numerical simulation results. In the simulation problem, there are two types of materials: sawdust material and C45 steel material of the pressing screw. Since sawdust has indefinite particle sizes, the paper selects some typical sizes ranging from 0.1 - 0.6 mm, as shown in Figure 11, to build a simulation model. During the simulation, particles will be randomly selected by the software.

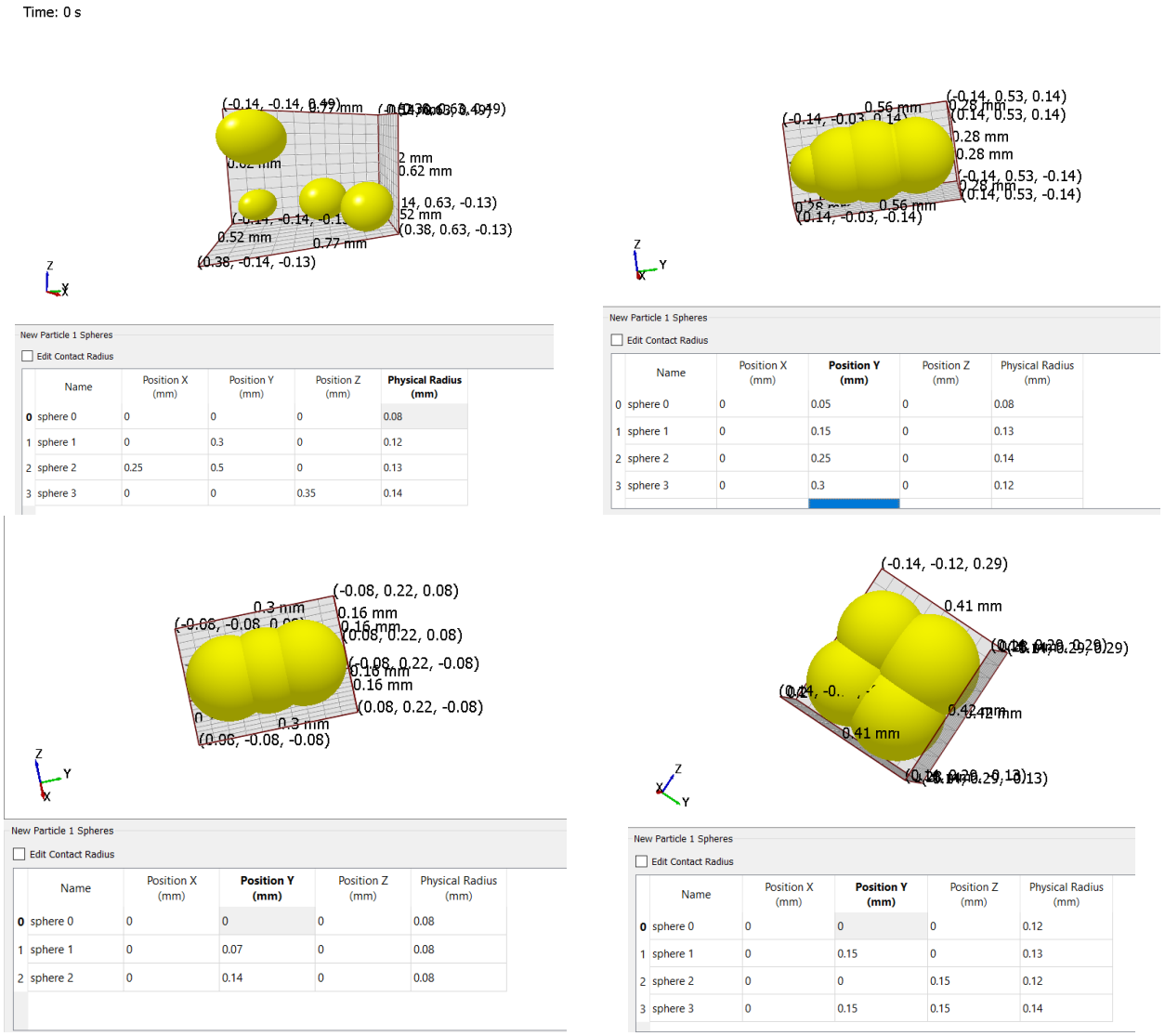

Fig. 11. Discrete material particle model.

The parameters of sawdust selected through real-world surveys are chosen as shown in Table 5 for simulation:

Table 5. Parameters of sawdust in the simulation model.

No	Parameter	Value
1	Total moisture	3 – 10%
2	Ash content	2 – 3%
3	Gross calorific value on air dried basic	4500 – 5000 Kcal/kg
4	Poison coefficient	0,1
5	Density	300 kg/m^3
6	Shear moduls	108 Pa
7	Thermal Conductivity	0,3 W/(m.K)
8	Conhesive Interactions	20 J/m^3

The parameters of pressing screw selected through real-world surveys are chosen as shown in Table 6 for simulation:

Table 6. Parameters of pressing screw in the simulation model

No	Parameter	Value
1	Thermal Conductivity	46,5 W/(m.K)
2	Geometry Temperature	220 - 280 (^{o}C)
3	Wear Constanst	0,005 Pa-1

c) Simulation results of factory pressing screws and optimal pressing screws

The simulation results of the wear of the two pressing screws at 11.5 seconds, 23.65 seconds, 35.75 seconds, 47.9 seconds, and 60 seconds are presented in Table 7 and graphically represented in Figure 12.

Table 7. Simulation results of wear values for the pressing screw over time.

Parameter	Wear (mm) at 11.5 seconds	Wear (mm) at 23.65 seconds	Wear (mm) at 37.75 seconds	Wear (mm) at 47.9 seconds	Wear (mm) at 60 seconds
Factory pressing screw	0.0117489	0.0253039	0.0388806	0.0539820	0.0687176
Optimal pressing screw	0.0007428	0.0019557	0.0033403	0.0046565	0.0057974

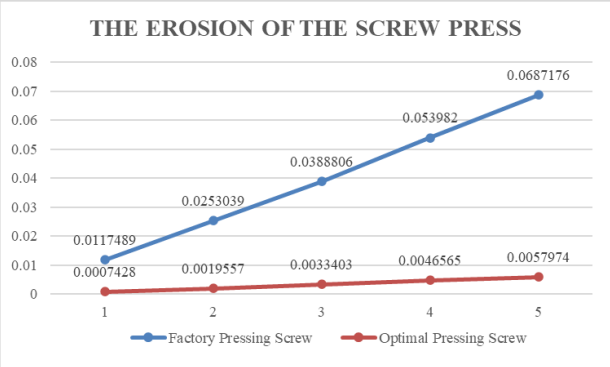

Fig. 12. Comparison of wear of factory pressing screw and optimal pressing screw.

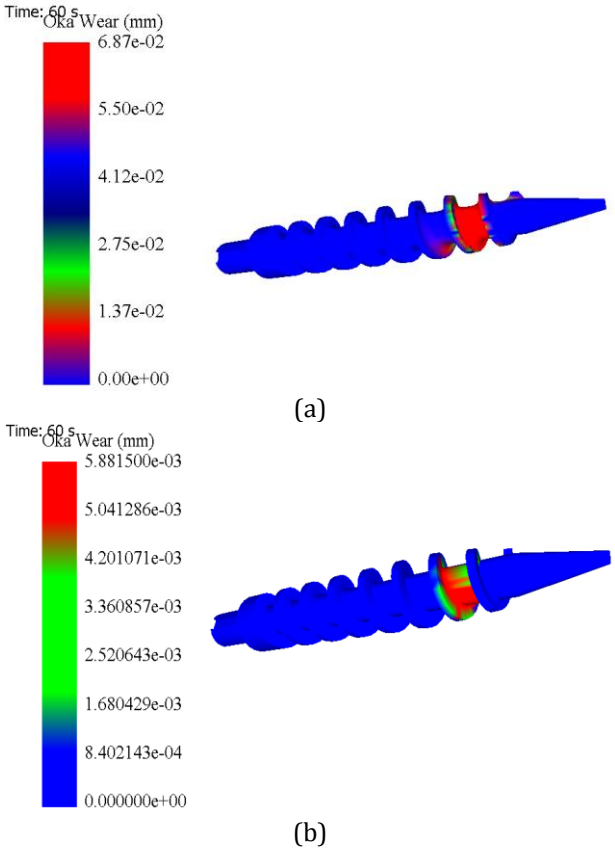

Fig. 13. Images of simulation results of the wear for the factory pressing screw (a) and optimal pressing screw (b).

It can be observed that during the operation, the pressing screw exhibits localized wear, primarily focusing on the region between the first and third crest width of the screw. However, when changing the profile of the pressing screw, the wear phenomenon is more evenly distributed, and the wear of the optimial pressing screw has significantly reduced compared to the wear of the factory pressing screw, as shown in the results in Figure 14. The optimal pressing screw's compression pressure has also decreased significantly from $6.62x10^5$ Pa to $2.46x10^5$ Pa, as shown in Figure 14a and Figure 14b, indicating that the factory pressing screw experiences greater wear than the optimal one.

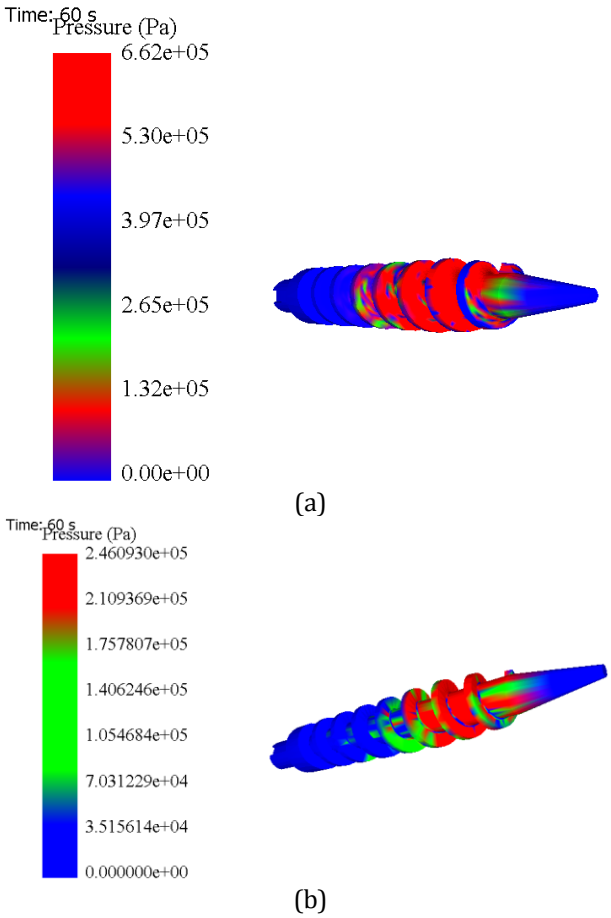

Fig. 14. Image of the simulation results of compression pressure for the factory pressing screw (a) and the optimal pressing screw (b).

Through our research, we have observed that during the operation, the pressing screw often experiences localized wear at specific locations.

However, after modifying the pressing screw profile according to the proposed optimization scheme, we have observed a more widespread distribution of wear phenomena. Notably, the wear of the optimal pressing screw has significantly decreased compared to the conventional factory pressing screw. This represents a crucial advancement, demonstrating that adjusting the profile of the pressing screw can be effective in reducing wear phenomena and enhancing the longevity of the pressing screw.

d) Experimental results at the factory

To validate the simulation results, we conducted experiments at the smokeless charcoal production factory. We continuously operated the pressing screw under the factory conditions, in which the pressing sawdust was mixed with the ratio of 2 parts sawdust from traditional villages to 1 part glue. We measured the working time until the product could no longer be extruded, then remove the screw, and measure the working time. The results are presented in Table 8.

Table 8. Experimental results at the factory.

No	Working time of factory pressing screw, (hours)	Working time of optimal pressing screw, (hours)	Increased life expectancy (%)
1	41	54	31,70
2	43	56	30,23
3	42	55	30,95
4	41	55	34,14
5	42	56	33,33
The average value	**42**	**55,2**	**32,07**

The screw cannot extrude the product due to changes in profile, wear, and deformation due to heat as shown in Figure 15.

Fig. 15. Image of worn and thermal deformation screw.

5. CONCLUSION

The numerical simulation results have provided detailed insights into the wear patterns of the pressing screw during smokeless charcoal production:

1. Reduction in wear:

- The average wear of the factory pressing screw and the optimal pressing screw decreased from 0.039266 mm to 0.00329854mm.
- The maximum wear at the same observed time for the factory pressing screw decreased from 0.0687176 mm to 0.0057974 mm.

2. Increase in working time:

- The initial results indicate that reducing wear leads to an increase in the working time of the pressing screw. This suggests significant potential for enhancing the longevity and efficiency of these devices.
- The experimental results show that the optimal pressing screw significantly increases its lifespan by an average of 32.07% compared to the factory pressing screw. In addition, the product quality of sawdust bars is guaranteed to meet the factory's requirements.

3. Theoretical foundation and creative design:

- This paper presents an innovative approach based on a robust theoretical foundation and the use of modern numerical simulations.
- By pinpointing the key wear-prone areas, this research provides optimal design solutions and surface improvement strategies for the pressing screw, thereby preventing wear and extending its operational lifespan.

4. Practical implications:

- This method not only serves as a theoretical foundation for other wear-prone components but also opens doors for new ideas in the production process.
- This creative application, coupled with modern numerical simulations, establishes a significant framework, bridging the gap between theory and practice. It offers precise and effective technical solutions for combating wear in the smokeless charcoal production process in Vietnam.

Acknowledgement

We would like to thank Hanoi University of Industry for providing funding for the research team according to the scientific research and technology development contract with contract code 02-2023-RD/HD-DHCN.

REFERENCES

[1] G. Müller and J. Senior, "Simplified theory of Archimedean screws," *Journal of Hydraulic Research*, vol. 47, no. 5, pp. 666–669, Sep. 2009, doi: 10.3826/jhr.2009.3475.

[2] M. Matúš, P. Križan, J. Ondruška, Ľ Šooš, "Analysis of tool geometry for screw extrusion machines. In: Proceedings of Aplimat", in 10th *International Conference Aplimat*, Bratislava, Slovakia, 2011, pp. 415-425.

[3] P. Križan, Mi. Matúš, Ľ. Šooš, J. Beniak, "Relationship between technological and material parameters during densification of beech sawdust", in *4th International Conference on Energy Systems, Environment, Entrepreneurship and Innovation*, Dubai, United Arab Emirates, 2015, pp. 278-285.

[4] A. S. Zidan, L. Kotamarthy, R. Ramachandran, M. Ashraf, and T. O'Connor, "Optimization of screw design for continuous wet granulation: A case study of metoprolol succinate ER tablets," *International Journal of Pharmaceutics*, vol. 623, p. 121964, Jul. 2022, doi: 10.1016/j.ijpharm.2022.121964.

[5] D. Kretz, S. Callau-Monje, M. Hitschler, A. Hien, M. Rädle, and J. Hesser, "Discrete element method (DEM) simulation and validation of a screw feeder system," *Powder Technology*, vol. 287, pp. 131–138, Jan. 2016, doi: 10.1016/j.powtec.2015.09.038.

[6] L. Pezo *et al.*, "Discrete element model of particle transport and premixing action in modified screw conveyors," *Powder Technology*, vol. 336, pp. 255–264, Aug. 2018, doi: 10.1016/j.powtec.2018.06.009.

[7] A. Hassanpour and M. Pasha, "Discrete element method applications in process engineering," in *CRC Press eBooks*, 2019, pp. 333–370. doi: 10.1201/9780429451010-9.

[8] M. Kremmer, "A discrete element method for industrial granular flow applications," Ph.D. dissertation, Dept. Agricultural & Environmental Science, Newcastle Univ, Newcastle upon Tyne, UK, 2001.

[9] H. Zhu, Z. Zhou, R. Yang, and A. Yu, "Discrete particle simulation of particulate systems: Theoretical developments," *Chemical Engineering Science*, vol. 62, no. 13, pp. 3378–3396, Jul. 2007, doi: 10.1016/j.ces.2006.12.089.

[10] X. Zhang and L. Vu-Quoc, "Modeling the dependence of the coefficient of restitution on the impact velocity in elasto-plastic collisions," *International Journal of Impact Engineering*, vol. 27, no. 3, pp. 317–341, Mar. 2002, doi: 10.1016/s0734-743x(01)00052-5.

[11] C. Wassgren and A. Sarkar, "Discrete element method (DEM) course module", Purdue University, 2008. [Online]. Available: https://pharmahub.org/resources/113.

[12] A. Grima et.al., "Predicting bulk flow and behaviour for design and operation of handling and processing plants," in *11th International Congress on Bulk Materials Storage, Handling and Transportation*, Newcastle, Australia, 2013, pp.1-10.

[13] J. F. Archard, "Contact and rubbing of flat surfaces," *Journal of Applied Physics*, vol. 24, no. 8, pp. 981–988, Aug. 1953, doi: 10.1063/1.1721448.

[14] *Standard Test Method for Scratch Hardness of Materials Using a Diamond Stylu*, ASTM G171-03, 2017, doi: 10.1520/G0171-03R17.

[15] F. Schramm, Á. Kalácska, V. Pfeiffer, J. Sukumaran, P. De Baets, and L. Frerichs, "Modelling of abrasive material loss at soil tillage via scratch test with the discrete element method," *Journal of Terramechanics*, vol. 91, pp. 275–283, Oct. 2020, doi: 10.1016/j.jterra.2020.08.002.

[16] *Standard test method for measuring abrasion using the dry sand/rubber wheel apparatus*, ASTM G65-16, 2021, doi: 10.1520/G0065-16R21.

[17] Y. Oka, K. Okamura, and T. Yoshida, "Practical estimation of erosion damage caused by solid particle impact," *Wear*, vol. 259, no. 1–6, pp. 95–101, Jul. 2005, doi: 10.1016/j.wear.2005.01.039.

[18] Y. Oka and T. Yoshida, "Practical estimation of erosion damage caused by solid particle impact," *Wear*, vol. 259, no. 1–6, pp. 102–109, Jul. 2005, doi: 10.1016/j.wear.2005.01.040.

[19] R. A. K. Editor-In-Chief, "Materials handling handbook," in *Wiley eBooks*, 1985. doi: 10.1002/9780470172490.

[20] M.P. Alekxandrop, *Podgiemno-transportnue masinu*, Masinostroenhie, Maskova, 1984.